Circ_Lrp6, a Circular RNA Enriched in Vascular Smooth Muscle Cells, Acts as a Sponge Regulating miRNA-145 Function

Ignacio Fernando Hall,* Montserrat Climent,* Manuela Quintavalle, Floriana Maria Farina, Tilo Schorn, Stefania Zani, Pierluigi Carullo, Paolo Kunderfranco, Efrem Civilini, Gianluigi Condorelli, Leonardo Elia

Rationale: **microRNAs (miRNAs) modulate gene expression by repressing translation of targeted genes. Previous work has established a role for miRNAs in regulating vascular smooth muscle cell (VSMC) activity. Whether circular RNAs are involved in the modulation of miRNA activity in VSMCs is unknown.**

Objective: **We aimed to identify circular RNAs interacting with miRNAs enriched in VSMCs and modulating the cells' activity.**

Methods and Results: **RNA sequencing and bioinformatics identified several circular RNAs enriched in VSMCs; however, only one, possessing multiple putative binding sites for miR-145, was highly conserved between mouse and man. This circular RNA gemmed from alternative splicing of Lrp6 (lipoprotein receptor 6), a gene highly expressed in vessels and implicated in vascular pathologies and was thus named circ_Lrp6. Its role as a miR-145 sponge was confirmed by determining reciprocal interaction through RNA immunoprecipitation, stimulated emission depletion microscopy, and competitive luciferase assays; functional inhibition of miR-145 was assessed by measuring expression of the target genes ITGβ8 (integrin-β8), FASCIN (fascin actin-bundling protein 1), KLF4 (Kruppel-like factor 4), *Yes1* (YES proto-oncogene 1), and *Lox* (lysyl oxidase). The interaction was preferentially localized to P-bodies, sites of mRNA degradation. Using loss- and gain-of-function approaches, we found that circ_Lrp6 hindered miR-145-mediated regulation of VSMC migration, proliferation, and differentiation. Differential expression of miR-145 and circ_Lrp6 in murine and human vascular diseases suggests that the ratio of circ_Lrp6 bound to miR-145 versus unbound could play a role in vascular pathogenesis. Viral delivery of circ_Lrp6 shRNA prevented intimal hyperplasia in mouse carotids.**

Conclusions: **circ_Lrp6 is an intracellular modulator and a natural sponge for miR-145, counterbalancing the functions of the miRNA in VSMCs. (*Circ Res*. 2019;124:498-510. DOI: 10.1161/CIRCRESAHA.118.314240.)**

Key Words: alternative splicing ■ circular RNA ■ epigenomics ■ gene expression ■ microRNAs ■ smooth muscle cells ■ vascular diseases

Approximately 90% of the mammalian genome is transcribed into noncoding RNAs (ncRNAs).[1,2] Over the last decade, the most studied category of ncRNAs has been that of the microRNAs (miRNAs or miRs). They have been shown to be involved in the control of many biological processes, including some leading to cardiovascular disease.[3] For instance, in vascular smooth muscle cells (VSMCs), the miR-143/145 cluster regulates the phenotypic switch from proliferation to differentiation; indeed, miR-145 is one of the most expressed miRNAs in VSMCs and its level of expression is directly associated with the extent of differentiation.[4–9] MiR-145 can also be transferred from VSMCs to endothelial cells and vice versa, playing specific biological functions in the receiving cells, in particular regulating cell growth and angiogenesis in the latter.[10,11]

Editorial, see p 456
Meet the First Author, see p 452

ncRNAs longer than 200 bp—defined as long ncRNAs—have been less studied to date than miRNAs; however, their roles in cardiovascular biology and disease is becoming ever more evident (reviewed in[1,12]). Recently, it was demonstrated that long ncRNAs can form loops of RNA.[13] These molecules—named circular RNAs (circRNAs)—derive from a noncanonical

Original received October 10, 2018; revision received November 20, 2018; accepted November 28, 2018. In October 2018, the average time from submission to first decision for all original research papers submitted to *Circulation Research* was 14.86 days.

From the Humanitas Research Hospital, Rozzano, Milan, Italy (I.F.H., M.C., M.Q., F.M.F., T.S., S.Z., P.C., P.K., E.C., G.C., L.E.); Humanitas University, Rozzano, Milan, Italy (I.F.H., S.Z., P.C., E.C., G.C.); Institute of Genetics and Biomedical Research, National Research Council, Rozzano, Milan, Italy (P.C., G.C., L.E.); and Department of Molecular and Translational Medicine, University of Brescia, Italy (L.E.).

*These authors contributed equally to this article.

The online-only Data Supplement is available with this article at https://www.ahajournals.org/doi/suppl/10.1161/CIRCRESAHA.118.314240.

Correspondence to Gianluigi Condorelli, MD, PhD, Humanitas Research Hospital, Via Manzoni 113, 20089 Rozzano (MI), Italy, Email gianluigi.condorelli@hunimed.eu; or Leonardo Elia, PhD, Department of Molecular and Translational Medicine, University of Brescia, Viale Europa 11, 25123 Brescia, Italy. Email leonardo.elia@unibs.it

Novelty and Significance

What Is Known?

- MiR-145 regulates vascular smooth muscle cell (VSMC) physiology and homeostasis.
- Modulation of miR-145 is involved in the development of atherosclerosis and arterial restenosis.
- Circular RNAs (circRNAs) are loops of RNA that can act as endogenous miRNA sponges.

What New Information Does This Article Contribute?

- Circ_Lrp6 is a circRNA enriched in VSMCs.
- Circ_Lrp6 modulates VSMC phenotypic switching by binding to miR-145, regulating its activity.
- Decreasing circ_Lrp6 expression is beneficial in a mouse carotid artery stenosis model.

In this study, we identified several circRNAs enriched in human and mouse vascular smooth muscle cells. We then searched for binding sites for VSMC-enriched miRNAs on these circRNAs. We identified only one circRNA conserved in human and mouse that potentially interacted with miR-145: circ_Lrp6 controlled VSMC migration, proliferation, and differentiation capacities through the interaction with miR-145, regulating its availability and, thus, its activity on targeted genes. Interaction between circ_Lrp6 and miR-145 takes place preferentially at cytoplasmic loci known as P-bodies. Circ_Lrp6 and miR-145 are expressed also in normal and diseased human arteries, with circ_Lpr6 being stable in disease. Modulation of circ_Lrp6 in a mouse model of vascular stenosis improved disease outcome. These findings provide insights on the role of circRNAs in the fine-tuning of vasculature regulation.

Nonstandard Abbreviations and Acronyms

AGO2	argonaute 2
ApoE	apolipoprotein E
circRNA	circular RNA
ITGβ8	integrin-β8
KLF4	Kruppel-like factor 4
LDL	low-density lipoprotein
Lox	lysyl oxidase
Lrp6	lipoprotein receptor 6
miR	microRNA
ncRNAs	noncoding RNAs
qPCR	quantitative polymerase chain reaction
PDGF-BB	platelet-derived growth factor
shRNA	short hairpin RNA
STED	stimulated emission depletion microscopy
TGF-β	transforming growth factor β
VSMC	vascular smooth muscle cell
Yes1	YES proto-oncogene 1

type of splicing defined as tail-to-head, because it goes from a downstream 5′ splice site to an upstream 3′ splice site,[14] a process suggested to be guided by specific repetitive sequences, such as *Arthrobacter luteus* sequences present on the flanking regions of the long ncRNA.[15,16] CircRNAs can derive from introns and exons, playing different biological roles on the basis of their genomic origin.[13,17–19] In particular, exonic circRNAs may regulate gene expression by directly binding to miRNAs: for instance, it has been shown that CDR1as (cerebellar degeneration-related protein 1 antisense RNA) has over 70 binding sites for miR-7, acting as a natural sponge for this miRNA and, thereby, able to modulate its activity on target genes.[14,20] In addition, the structure of circRNAs makes them resistant to RNase H exonuclease activity and enriches them in exosomes.[21]

Whether circRNAs are associated with cardiovascular diseases is largely unknown. Similarly, although the mechanisms through which miRNAs regulate VSMC biology have been clarified, whether they interact with other ncRNAs in this cell type is unknown. Thus, for the present study, we used RNA sequencing followed by bioinformatics analysis to determine the existence of hitherto unknown ncRNAs in VSMCs. Among the numerous ncRNAs identified, we found several circRNAs that could potentially bind to miRNAs enriched in VSMCs; however, only one, with multiple miRNA-145 binding sites, was conserved between mouse and humans. Of note, loss- and gain-of-function experiments revealed that this circRNA modulated the function of miR-145 and, thus, had an ability to regulate VSMC biology.

Methods

Data Availability

The RNA-sequencing dataset is available from the Gene Expression Omnibus database (http://www.ncbi.nih.gov/geo/) under accession number GSE99318.

The authors declare that all data supporting the findings of this study are available within the article and its Online Data Supplement.

CircRNA Identification

To systematically detect back-splice junctions in STAR mapped reads, we used DCC[22] with the following parameters: -Pi; -F; -M; -Nr 2 2;-fg; with at the least 2 counts in 2 biological replicates.

The full list of all *Mus musculus* circRNAs was downloaded from http://www.circbase.org/. UCSC Batch Coordinate Conversion (liftOver tool (https://genome.ucsc.edu/cgi-bin/hgLiftOver) was used to convert mm 9 to mm 10 genome coordinates. Complete overlap of all known circRNAs and CircCoordinates DCC output was computed with Bedtools intersect –f1 option, resulting in >250 annotated circRNAs.

To identify putative binding sites of VSMC-enriched miRNAs in the identified list of circRNAs, fasta file was obtained and searched for at least 2 pattern sequences specific for (seed sequences downloaded from targetscan.org): miR-145-5p (seed sequence: ACTGGAC); miR-143-3p (seed sequence: CATCTCT); miR-221-3p/222-3p (seed sequence: TGTAGCT); miR-21-5p (seed sequence: TAAGCTA); miR-29-3p (seed sequence: GGTGCTA); miR-26-5p (seed sequence: ACTTGAA); miR-133a-3p (seed sequence: GGACCAA); and miR-1-3p (seed sequence: CATTCCA). A complete list of the identified circRNAs is available in the Online Data Supplement section.

Animal Models

Please consult supplemental material.

Human Samples

Please consult in the Online Data Supplement. The protocol was approved by the institutional ethics committee (ICH-967); informed

consent was obtained from each patient in compliance with European Union and Italian laws.

In Situ Hybridization

The in situ protocol was performed as previously described with minor modifications.[11] Briefly, circ_Lrp6 was designed to cover the junction site of the circRNA (specific sequences of the probe and the scrambled counterpart are listed in Online Table I) and synthetized as single-strand DNA oligonucleotides conjugated with digoxigenin by integrated DNA technologies. The miR-145-5p and miRNA scrambled probes (digoxigenin- and Cy3-labeled) were purchased from Exiqon (respectively, catalog no. YD00616648-BCG and YD00616648-BCC). Cells or tissues were fixed in 4% paraformaldehyde (tissues then embedded in optimal cutting temperature compound) and permeabilized with 0.3% Triton in PBS for cells, while tissues were treated with proteinase K (Exiqon). Samples were then blocked with PBS, 0.1% Tween, 1% BSA, 2% fetal bovine serum, and hybridization was performed on at 58°C, diluting the probes in miRNA ISH buffer (Exiqon) at the following concentrations: miR-145 or miRNA scrambled, 20 nmol/L and circ_Lrp6 of circ_scrambled, 100 nmol/L. For the detection of digoxigenin-labeled probes, samples were incubated with anti-digoxigenin-HRP antibody and the signal amplified using the Alexa Fluor 647 Tyramide Reagent (Life Technologies). Following the in situ protocol, immunofluorescence was performed to assess the cellular localization of the ncRNAs as previously described.[9] The utilized antibodies were ACTA2 (Sigma-Aldrich, catalog no. A5228) or DCP1A (Abcam, Catalog no. AMAB183709). Diamond Prolong (Life Technologies) was used as mounting medium. Background was determined on the signals observed with the specific scrambled probes for the in situ and the secondary antibody alone for the immunofluorescence.

Super-Resolution Confocal Imaging

Stimulated emission depletion (STED) xyz images were acquired in unidirectional mode with a Leica SP8 STED3X confocal microscope system. 4′, 6-diamidino-2-phenylindole was excited with a 405 nm diode laser and emission collected from 406 to 480 nm; Cy3 was excited with a 488 nm-tuned white light laser and emission collected from 490 to 620 nm; Alexa Fluor 647 was excited with a 647 nm-tuned white light laser and emission collected from 650 to 800 nm. Line sequential acquisition was applied to avoid fluorescence overlap. Gating was applied between 0.3 and 6 ns to avoid collection of reflection and autofluorescence. A 775 nm pulsed-depletion laser was used for Cy3 excitations (100% of power) and Alexa Fluor 647 excitations (30% of power). Images were acquired with a Leica HC PL APO CS2 100×/1.40 oil STED white objective. Gated pulsed-STEDs were applied to the Cys3 and Alexa Fluor 647 fluorophores. Collected images were deconvolved with Huygens Professional software and analyzed with Fiji software.

Cell Cycle Analysis

This was conducted as previously described, with minor modifications.[23] Briefly, cells (1×10^6) were detached from the plate and washed twice with PBS, fixed in 70% ethanol and kept at 4°C before overnight DNA staining with 2.5 µg/mL propidium iodide (Calbiochem) in the presence of 12.5 µg/mL RNase (LifeTechnologies). The number of cells at each stage of the cell cycle was measured using a BD FACSCanto II flow cytometry system (BD Bioscience).

Statistical Analysis

Prism software (GraphPad Software) was used to assess data normality and for statistical calculations. Statistical calculations were performed on at least 3 independent experiments. For in vivo and in vitro experiments with >5 biological replicates, data normality was calculated with the Kolmogorov-Smirnov test. Statistical analyses were then performed with 2-tailed *t* test (parametric unpaired or paired, 2 group of analysis), Wilcoxon test (nonparametric paired, 2 group of analysis), Mann-Whitney *U* test (nonparametric unpaired), or repeated-measures ANOVA combined with Tukey multicomparison (comparisons between >2 groups, parametric unpaired). Data are represented as mean±SD unless otherwise stated. A value of $P\leq0.05$ was considered to be statistically significant.

An extended methods section is available in the Online Data Supplement section.

Results

Bioinformatics Identifies circRNAs Enriched in VSMCs

It is established that circRNAs can act as endogenous miRNA sponges.[14,20] Thus, to further define the panorama of ncRNA activity and interaction in VSMCs, we searched for circRNAs that were conserved between human and mouse and that had potential binding sites for miRNAs enriched in this cell type. To this end, we first exploited a published transcriptome profiling dataset of human VSMCs.[24] To identify robustly expressed circRNAs shared in all biological replicates, we implemented STAR mapping alignment[25] with DCC, a Python package intended to detect and quantify circRNAs with high specificity.[26] Integration with annotated circRNAs collated on the circBase database lead to the identification of 7770 circRNAs, which were mainly clustered in superfamilies (Online Figure I; Online File I). Using the RefSeq database,[27] we then annotated these circRNAs, observing that >80% of them consisted of protein-coding exons, whereas smaller fractions aligned with introns and intergenic regions of genes (Figure 1A).

To assess whether human and mouse VSMCs shared similar circRNA signatures, we profiled three biological replicates of mouse aorta (intimal and adventitial layers were surgically removed before RNA extraction) with RNA-sequencing technology. Total RNA was mapped with the STAR algorithm to the UCSC *M musculus* reference genome (build mm 10), slightly adjusted for the specific identification of chimeric reads and back-splice junctions. On average, >50 million paired reads were mapped in each replicate. DCC was then applied to detect and quantify putative circRNAs shared in all 3 replicates. Although the circBase database offers a less-extensive catalog of annotated mouse circRNAs with respect to those in human cells, we still found 256 circRNAs uniquely expressed in mouse VSMCs (Online Figure I; Online File I). These potential murine-derived circRNAs annotated similarly to the human ones (Figure 1B).

To evaluate whether previously identified human and mouse circRNAs contained conserved binding sites for miRNAs previously shown to be important in VSMC biology,[28] we first extracted putative spliced sequences and scanned for the presence of at least 2 binding sites for miR-145-5p, miR-143-3p, miR-221-3p/222-3p, miR-21-5p, miR-29-3p, miR-26-5p, miR-133a-3p, or miR-1-3p (Figure 1C). We identified several circRNAs with potential binding sites for these VSMC-enriched miRNAs (Figure 1D); however, among all these putative candidates, only one, with binding sites for miR-145-5p—one of the most expressed and biologically active ncRNAs regulating VSMCs[4–7]—was conserved between mouse and humans (Online Figure II).

This specifically conserved circRNA has already been classified as circ_1529 in mouse and circ_8932 in humans; in both species, it derives from the same coding gene, namely Lrp6 (LDL [low-density lipoprotein] receptor-related protein 6; Figure 1E). The circRNA—from here on designated as circ_Lrp6—has at least 7 binding sites for miR-145 (three

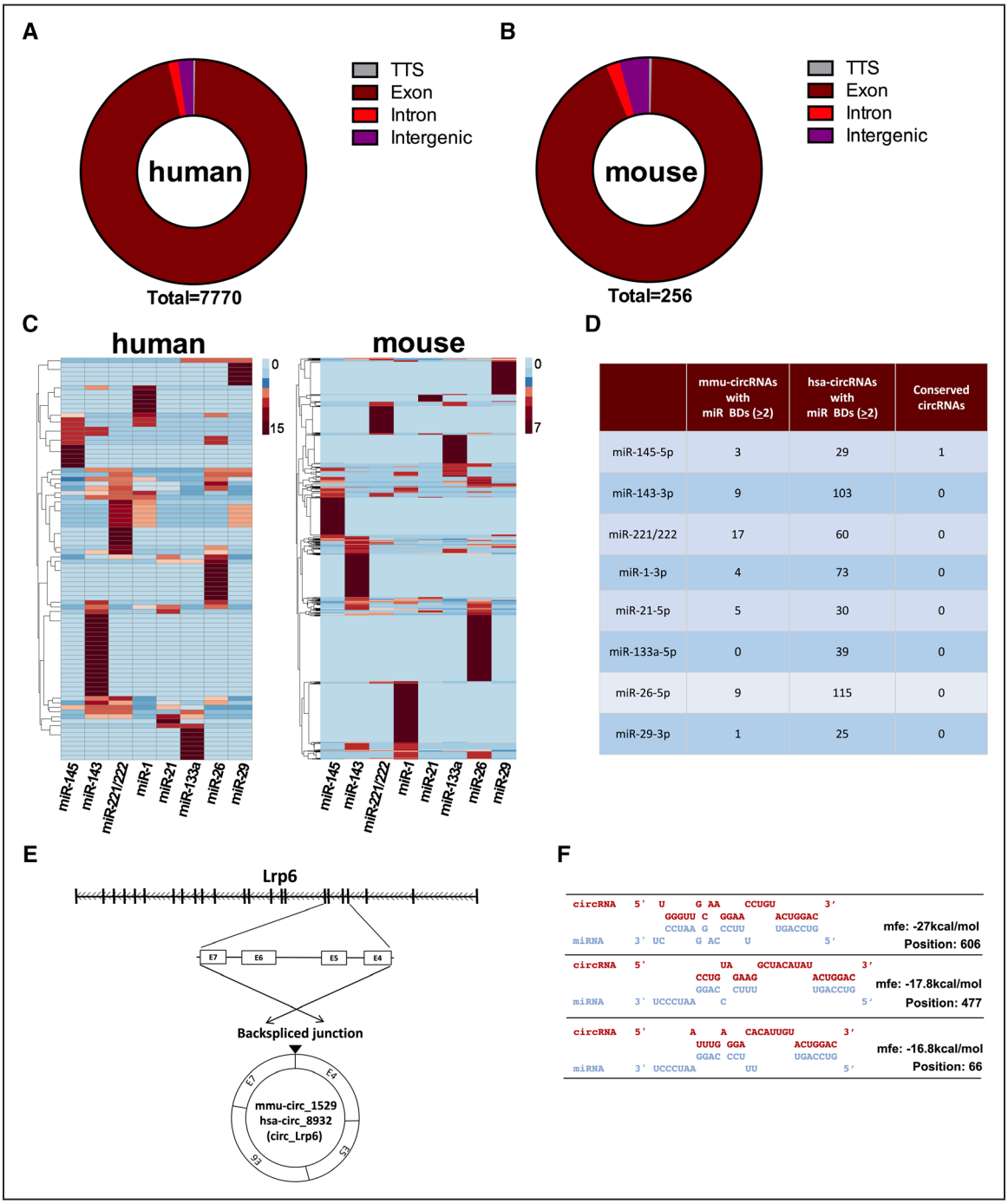

Figure 1. Profiling of circular RNAs (circRNAs) in human and mouse aortas. A and **B**, Genomic origin of identified circRNAs in humans and mouse, respectively. **C**, Heat maps for the identified circRNAs containing binding sites for the analyzed vascular smooth muscle cell (VSMC) enriched microRNAs (miRNAs). Color bars indicate number of miRNA binding sites. **D**, Number of human and mouse circRNAs containing the putative binding sites (BDs) for the analyzed miRNAs. **E**, Schematic of the back-spliced junction leading to multiple exons in mouse and human circ_LRP6. **F**, Thermodynamic analysis of the putative 8-mer interactions between circ_Lrp6 and miR-145. TTS indicates transcription termination sites.

8-mers and four 7-mers, the latter nonetheless with stable physical interactions; Figure 1F; Online Figure IIIA and IIIB), suggestive of an evolutionarily conserved biological function.

Validation of the VSMC-Enriched circRNA

We tested the existence and function of the predicted circRNA in mouse VSMCs. Specific head-to-tail splicing was evaluated by polymerase chain reaction (PCR) following reverse transcription (RT). Divergent primers produced amplicons from RNA-derived samples and not from genomic DNA (Figure 2A; Online Figure IVA). To rule out the possibility that this alternative splicing could have resulted from trans-splicing or genomic rearrangement, or that the results were PCR artifacts, we further validated our results as follows. Because RNase R preferentially degrades linear RNA sequences,[29] we digested VSMC-derived RNA with this enzyme and quantified the resistance of circ_Lrp6,

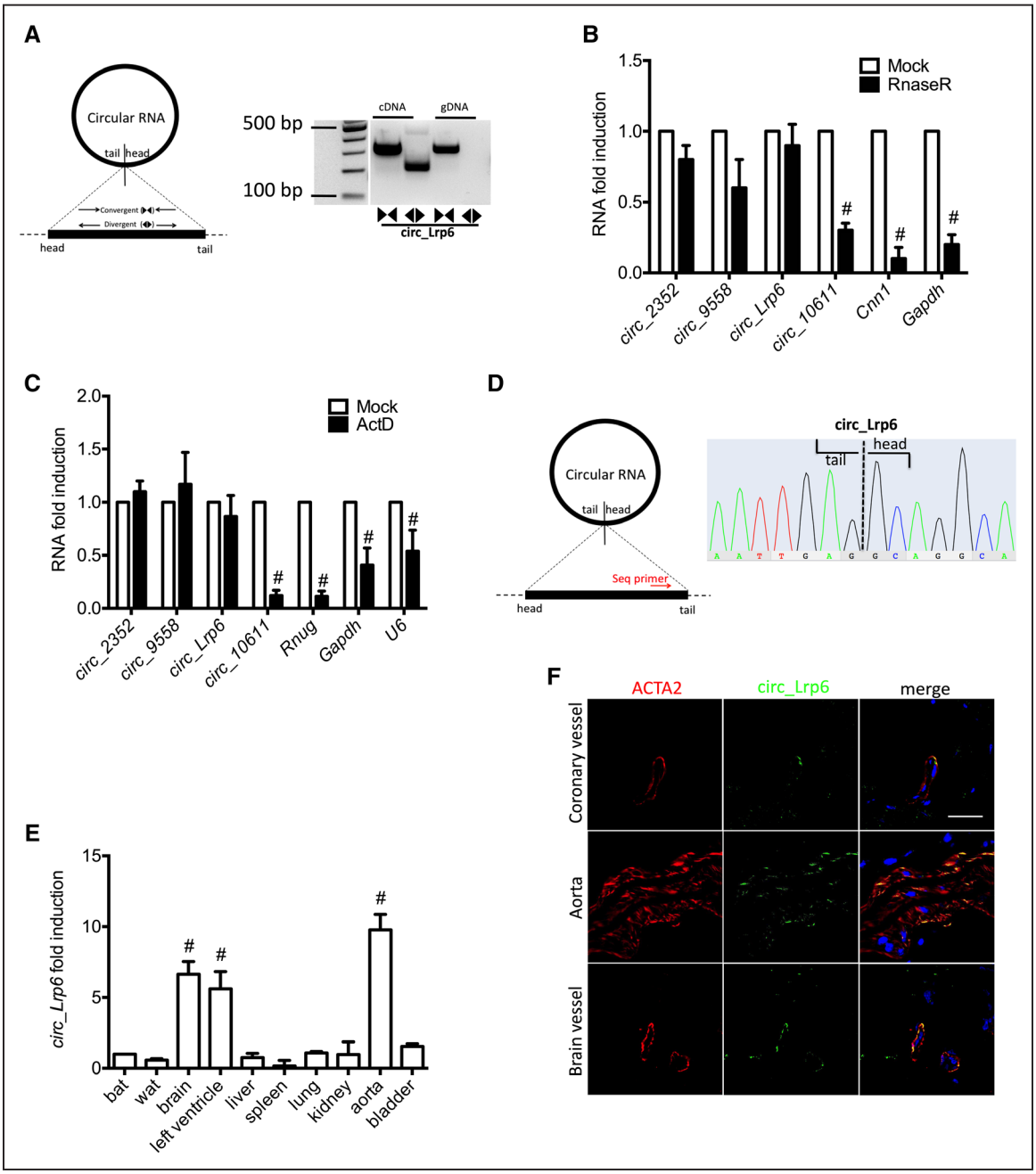

Figure 2. Validation of circ_Lrp6. A, Divergent primers amplify circ_Lrp6 in cDNA but not genomic DNA (gDNA). Size marker in base pairs. **B**, Circular RNAs (CircRNAs) are at least 10-fold more RNase R-resistant than calponin (*Cnn1*) and glyceraldehyde 3-phosphate dehydrogenase (*Gapdh*) mRNAs and (**C**) stable after 24 h of transcription block with actinomycin D (ActD). **D**, Sanger sequencing of the amplified band with divergent primers confirms head-to-tail splicing. **E**, *Circ_Lrp6* distribution in mouse tissues analyzed by reverse transcription quantitative polymerase chain reaction (RT-qPCR). **F**, In situ hybridization for circ_Lrp6 in mouse tissues: brain, heart, and aorta. In this experiment, actin (ACTA2) was detect using a secondary antibody labeled with Alexa-488, while for circ_Lrp6 we used a digoxigenin (DIG)-labeled probe and the signal amplified using the tyramide-Alexa_647 system. Scale bar: 50 μm. Data are the average of at least 3 independent experiments, and error bars indicate SD. To compare means, 2-tailed Student *t* test was used in **B** and **C**, and 1-way ANOVA in **E**; #*P*<0.05. bat indicates brown adipose tissue; and wat, white adipose tissue.

together with other three potential circRNAs, by quantitative PCR (qPCR): 3 out of 4 were at least 8× more resistant than linear control mRNAs, such as *Calponin* and *Gapdh* (Figure 2B). Moreover, since circRNAs have a longer turn-over when compared with linear mRNAs,[14] we tested *circ_Lrp6* expression after blocking transcription: exposure to actinomycin D for 24 hours reduced the stability of linear mRNAs and short ncRNAs but did not alter the expression of *circ_Lrp6* (Figure 2C). Moreover, Sanger DNA sequencing confirmed head-to-tail splicing on these samples (Figure 2D; Online Figure IVB).

We then evaluated *circ_Lrp6* expression in mouse tissues by RT-qPCR with divergent primers (Figure 2E). Localization in VSMCs was confirmed by in situ hybridization in tissues with the highest *circ_Lrp6* expression, that is, heart, brain, and aorta (Figure 2F). RNA sequencing confirmed expression in human thoracic aortas, although read enrichment was also observed

in the liver (Online Figure IVC). Of note, while *circ_Lrp6* and *Lrp6* were enriched in vessels (Figure 2E; Online Figure V), not all tissues expressed them together, suggesting the existence of differential gene expression regulation in different tissues.

Circ_Lrp6 Is a miR-145 Sponge

We reasoned that if circ_Lrp6 interacted with miR-145, they should colocalize. We, therefore, evaluated their localization in mouse primary VSMCs by in situ hybridization and nuclear/cytoplasmic fractionation. We found that both ncRNAs were highly enriched in the cytoplasm (Figure 3A and 3B).

We then assessed the effect of circ_Lrp6 on miR-145 activity. To this end, we generated a vector expressing the circRNA or relative controls (Online Figure VIA): transient transfection of HEK-293T cells with the circular construct, but not with the reverse or linear ones, induced the expression of the circRNA (Online Figure VIB); moreover, Northern blotting confirmed that the circular construct produced an ncRNA similar in size to the endogenous circ_Lrp6 of VSMCs (Online Figure VIC). To test the effect of circ_Lrp6 on miR-145 activity, we used a luciferase reporter carrying the 3′-untranslated region sequence of Itgβ8 (integrin β8), a gene we previously reported to be a miR-145 target.[11] In HEK-293T cells, overexpression of the circular construct blunted the negative effect of miR-145 on luciferase expression, whereas the reverse construct did not (Figure 3C; Online Figure VIIA).

To confirm the miR-145-dependent effect of circ_Lrp6 on Itgβ8, we designed a short hairpin (sh)RNA-sequence targeting circ_Lrp6 (Online Figure VIIB): 2 of the 3 clones inhibited circ_Lrp6 expression without having an effect on Lrp6 (Online Figure VIIC). We transfected primary VSMCs with 3′-untranslated region-Itgβ8 constructs expressing either the wild-type or a mutated miR-145 seed sequence.[11] As expected, luciferase activity was reduced in the circ_Lrp6 loss-of-function condition but not when the seed sequence was mutated (Figure 3D). This indicated that the effect of circ_Lrp6 on Itgβ8 was directly dependent upon the binding of miR-145 to the 3′-untranslated region of *Itgβ8* mRNA.

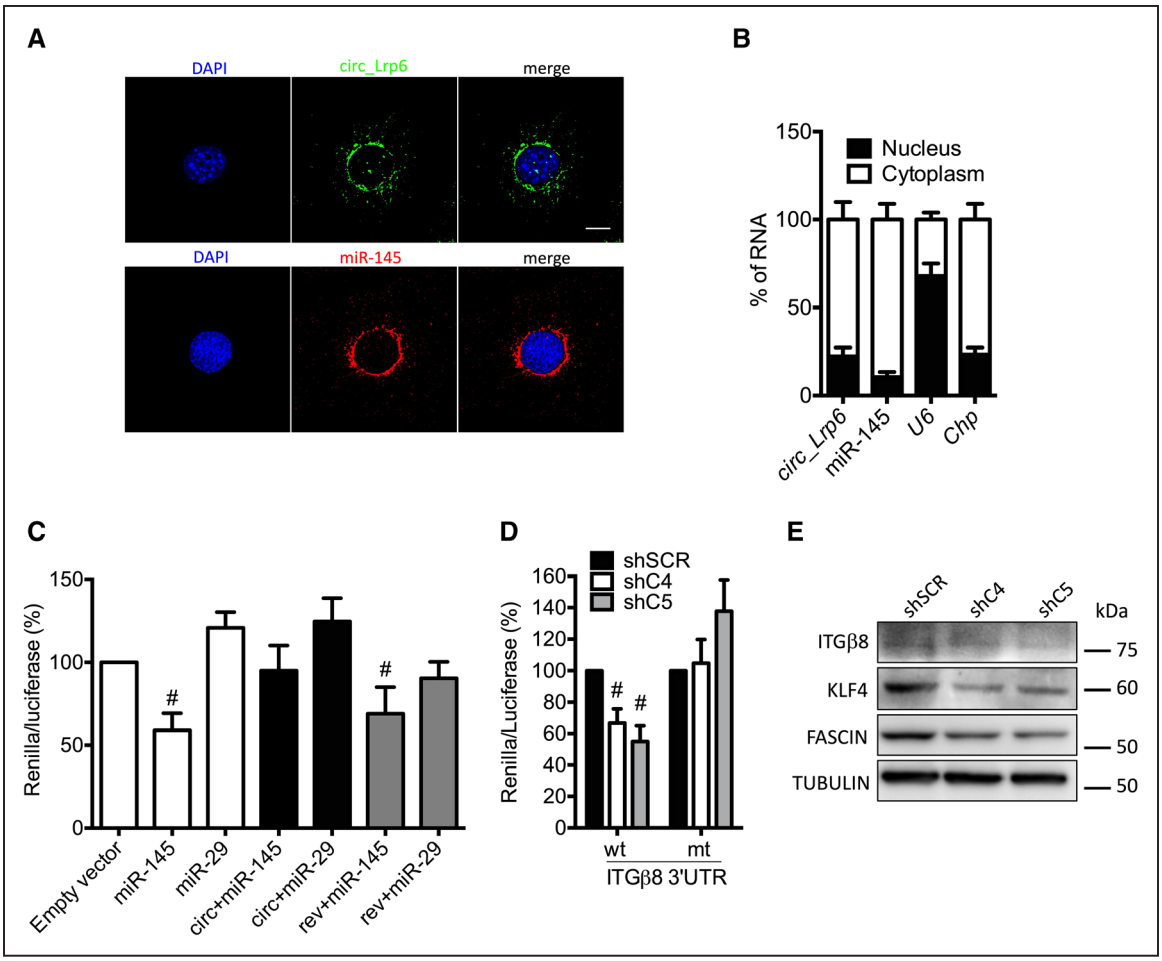

Figure 3. Circ_Lrp6 is a miR-145 sponge. A, In situ hybridization showing dispersed, cytoplasmic localization of circ_Lrp6 and miR-145 in vascular smooth muscle cells (VSMCs). We used digoxigenin (DIG)-labeled probes for both ncRNAs, amplifying the signals with the tyramide-Alexa_647 system. Scale bar: 10 μm. **B**, Reverse transcription quantitative polymerase chain reaction (RT-qPCR) analysis of *circ_Lrp6* and miR-145 expression in nuclear/cytoplasmic-fractionated RNAs. **C**, Luciferase reporter assays using reporter constructs for miR-145 together with *circ-Lrp6* constructs able to circularize (*circ*) or not (*rev*). HEK-293T cells were transfected in 12-well dishes with 0.5 μg of empty, miR-145, or miR-29 vectors plus *circ* or *rev* constructs together with 0.1 μg of a 3′-untranslated region (3′UTR)-ITGβ8 psiCheck2 reporter. The relative levels of renilla luminescence normalized to firefly luminescence are plotted. **D**, 3′UTR-Itgβ8 (integrin beta 8) luciferase reporter assays were performed in VSMCs in which wild-type (wt) or mutant (mt) constructs for the miR-145 seed sequence were transfected in control (scrambled shRNA [shSCR]) or *circ_Lrp6*-silenced (shC4 and shC5) VSMCs. **E**, Representative Western blots for known miR-145 targets in *circ_Lrp6*-silenced (shC4 and shC5) and control (shSCR) VSMCs. ITGβ8, FASCIN, and KLF4 (Kruppel-like factor 4) protein levels are reduced in *circ_Lrp6*-silenced VSMCs. Data are the average of at least 3 independent experiments, and error bars represent SD. To compare means, 1-way ANOVA was used in **C** and **D**; #$P<0.05$.

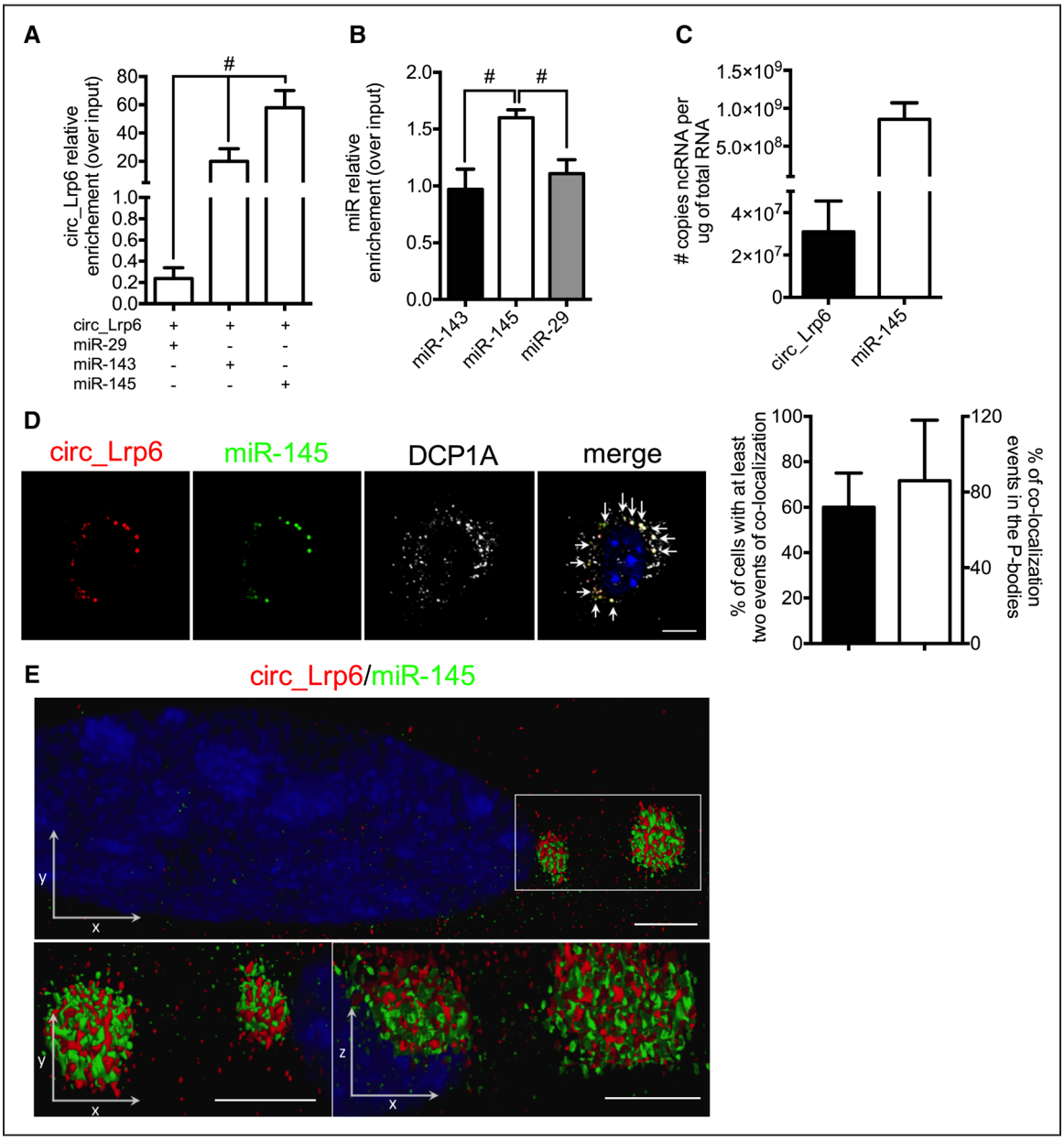

Figure 4. Direct interaction of Circ_Lrp6 with miR-145. A, Argonaute 2 (AGO2) immunoprecipitation in HEK-293T cells cotransfected with the circ constructs together with miR-145 or miR-143 and miR-29 as controls. Quantitative polymerase chain reaction (qPCR) values obtained using divergent primers were normalized on the input and the IgG value subtracted. **B**, Reverse transcription (RT)-qPCR analysis of miR-143, miR-145, and miR-29 in *circ_Lrp6*-precipitated RNA. qPCR values obtained using specific miRNA primers were normalized on the input and values derived by the RNA-immunoprecipitation (IP) using a scrambled probe subtracted. **C**, Quantification of absolute copy number for *circ_Lrp6* and miR-145 in vascular smooth muscle cells (VSMCs). **D**, Double in situ hybridization and relative quantification on proliferative primary VSMCs for circ_Lrp6, miR-145, and immuno-fluorescence for DCP1A. In this experiment, we used a digoxigenin (DIG)-labeled probe for circ_Lrp6, amplifying the signal with the tyramide-Alexa_647 system; for miR-145, we used an LNA probe labeled with Cy3 dye, while for DCP1A, a secondary antibody labeled with Alexa_594 was used. White arrows indicate points of circ_Lrp6/miR-145/DCP1A colocalization. Scale bar: 10 μm. **E**, Z stack stimulated emission depletion microscopy (STED) acquisition of the same experiment described in **D**. Scale bars: 2 μm. Data are the average of at least 3 independent experiments and error bars represent SD. To compare means, 1-way ANOVA was used in **A**, 2-tailed Student *t* test in **B**; #$P<0.05$.

To further corroborate the effect of circ_Lrp6 on miR-145 activity, we reasoned that inhibition of the circRNA should induce downregulation of different miR-145 targets. Indeed, the presence of the short hairpin RNAs (shRNAs) targeting circ_Lrp6 reduced the protein level of known miR-145 targets, including ITGβ8,[11] FASCIN,[8] and KLF4 (Kruppel-like factor 4)[7] in primary mouse VSMCs (Figure 3E; Online Figure VIIIA through IIIC).

The binding of circRNAs to miRNAs is mediated by AGO2 (argonaute 2).[14] When we immunoprecipitated AGO2 from HEK-293T cells cotransfected with the circular constructs together with miR-145, pull-down of circ_Lrp6 was enriched versus controls (ie, miR-143/*circ* versus miR-29/*circ*), indicating that AGO2 mediates binding of circ_Lrp6 to miR-145 (Figure 4A; Online Figure IXA). Direct binding of the 2 ncRNAs was then validated by RNA immunoprecipitation, using a specific biotinylated probe

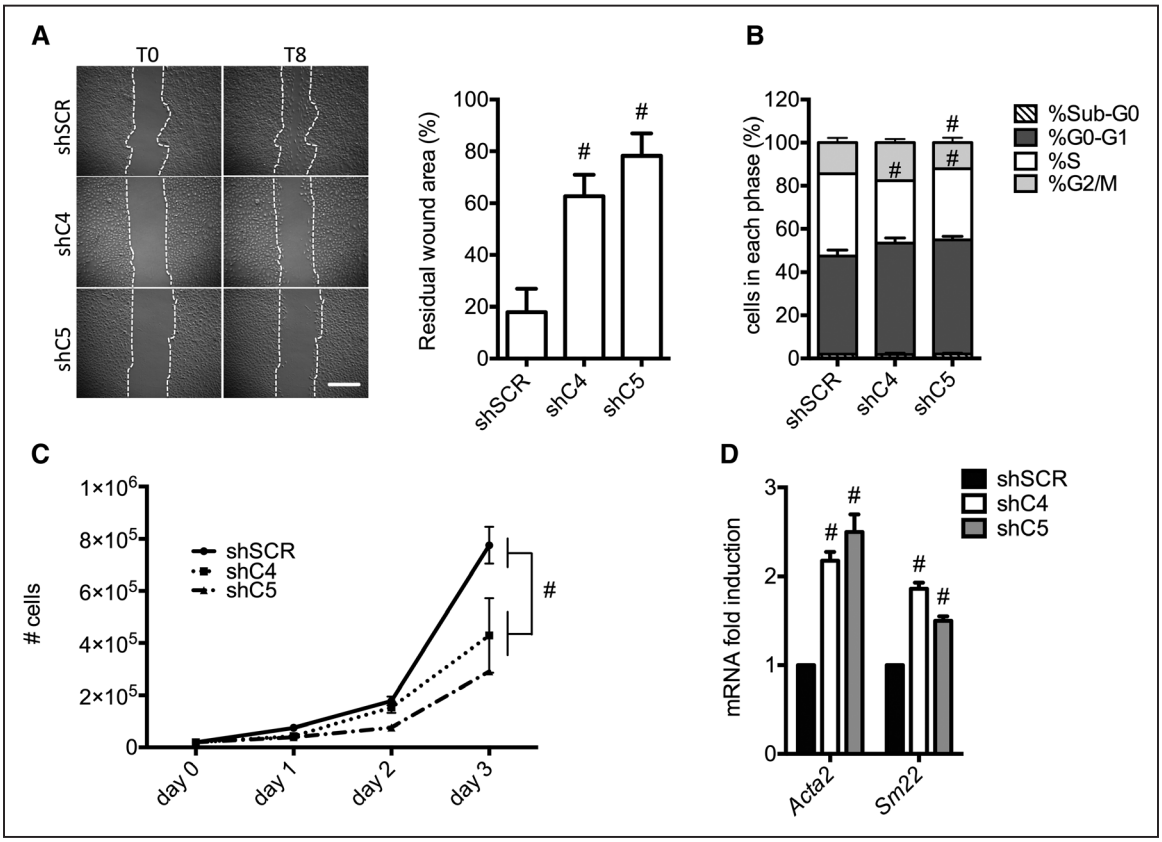

Figure 5. Biological effects of modulating circ_Lrp6 in vascular smooth muscle cells (VSMCs). A, Wound assay on *circ_Lrp6*-silenced VSMCs. The graph shows quantification of the residual wounded area 8 h postscratch vs scrambled shRNA (shSCR) controls (n=5). Scale bar: 250 μm. **B**, Cell cycle analysis of *circ_Lrp6*-silenced VSMCs vs shSCR controls. **C**, Cell growth curve of *circ_Lrp6*-silenced VSMCs vs shSCR controls (n=5). **D**, Expression of actin (*Acta2*) and transgelin (*Sm22*) in *circ_Lrp6*-silenced (shC4/5) vs control (shSCR) VSMCs, measured by reverse transcription quantitative polymerase chain reaction (RT-qPCR). Where not stated, data are the average of at least 3 independent experiments, and error bars represent SD. For **A** and **C**, data normality was calculated with Kolmogorov-Smirnov (K-S) test. To compare means, 1-way ANOVA was used in A–D; #$P<0.05$.

designed on the tail-to-head junction of circ_Lrp6. To this end, we grew VSMCs in medium containing 0.1% fetal bovine serum, which increases the levels of both ncRNAs (Online Figure IXB and IXC). Cells were then fixed, circ_Lrp6 enriched by immunoprecipitation, and the levels of miR-145, miR-143, and miR-29 measured by RT-qPCR. We found an increased amount of miR-145 in the *circ_Lrp6*-enriched RNA, strongly supporting the notion that these 2 ncRNAs directly interact (Figure 4B). We also quantified the absolute copy number of miR-145 and *circ_Lrp6* in primary mouse VSMCs (standard curves for the ncRNAs are given in Online Figure XA and XB). Considering that circ_Lrp6 has at least 7 binding sites for miR-145 (Online Figure IIIA and IIIB), the observed miRNA-145/circ_Lrp6 ratio seemed to be compatible with a sponge activity (Figure 4C).

Interaction between the 2 ncRNAs was further confirmed by in situ hybridization for circ_Lrp6 and miR-145 on isolated VSMCs, which indicated that an average of 60% of cells has at least 2 events of colocalization of the 2 ncRNAs. Furthermore, around 85% of these spots were located in processing bodies (P-bodies; Figure 4D; Online Figure XC), cytoplasmic loci known to be involved in mRNA decay controlled by miRNA activity,[30] but also where circular RNA can be found.[20] More importantly, physical interaction was demonstrated at the nanometric resolution scale by STED super-resolution microscopy (Figure 4E).

Altogether, these findings prove that circ_Lrp6 and miR-145 physically interact in VSMCs.

Biological Effects of circ_Lrp6 on VSMCs

We then evaluated the role on VSMC homeostasis, using functional assays in loss- or gain-of-function conditions. A wound-healing assay indicated significant reductions in VSMC migratory capacity when *circ_Lrp6* was silenced (Figure 5A). Silencing also reduced the percentage of VSMCs in the S phase of the cell cycle (Figure 5B), impairing proliferation (Figure 5C). Coherently with differentiated VSMCs being less migratory and proliferative,[31] and with upregulated miR-145 correlating with a prodifferentiation phenotype,[4,5,8] silencing of *circ_Lrp6* increased the VSMC differentiation markers smooth muscle actin and transgelin (Figure 5D).

To corroborate these findings, we performed rescue experiments in which miR-145 was inhibited in *circ_Lrp6*-silenced VSMCs (Online Figure XIA and XIB). To this end, we used a short hairpin sequence designed on the specific head/tail splicing site because it maps only to the circ_Lrp6 sequence. Inhibition of miR-145 was indeed able to reestablish the proliferative capacity, as well as the migratory and differentiation status, of primary VSMCs (Figure 6A through 6C). In addition, there was a recovery of the expression of miR-145 targets regulated at the RNA level, such as *Fascin*,[8]

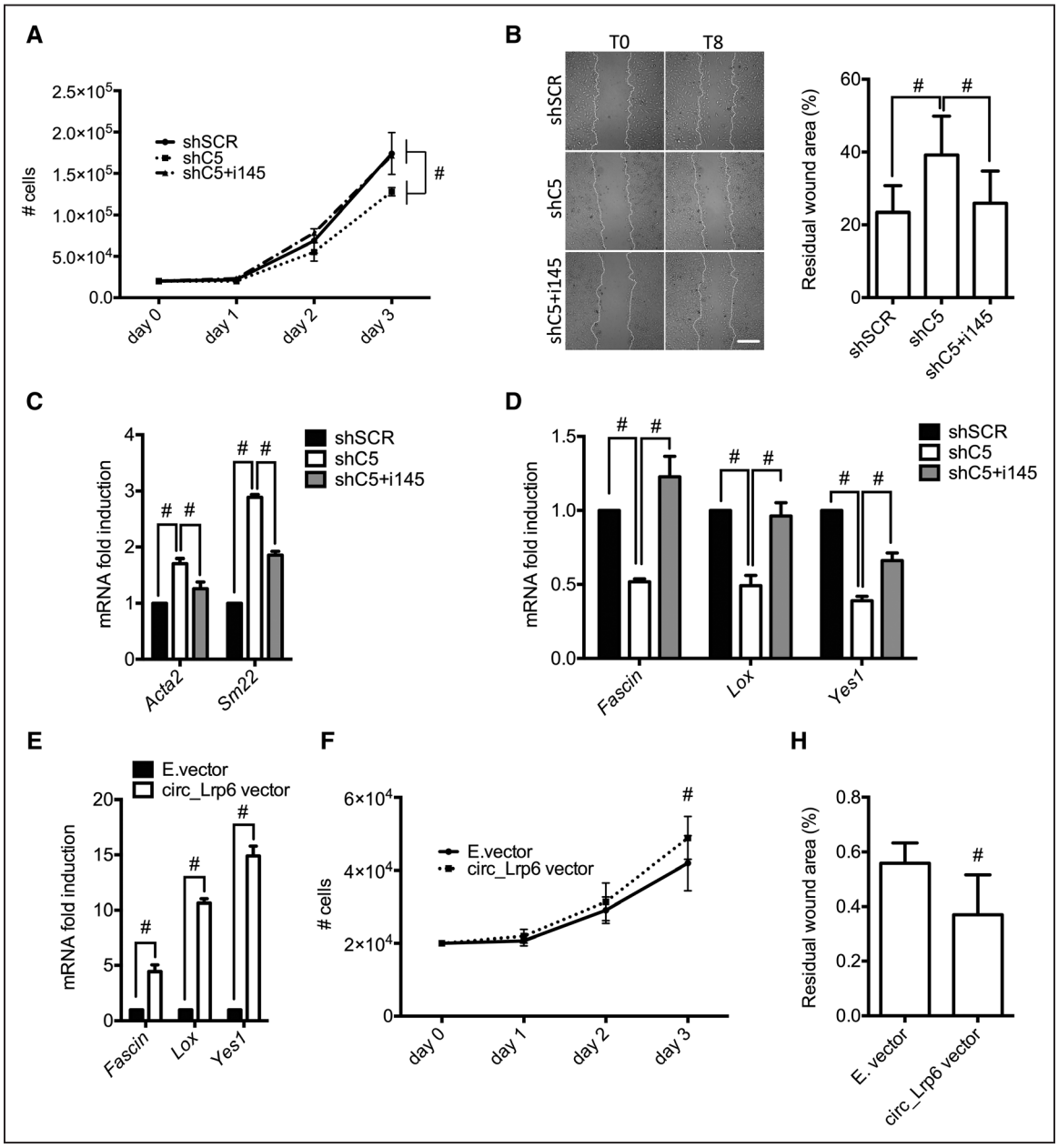

Figure 6. Inhibition of miR-145 in circ_Lrp6-silenced vascular smooth muscle cells (VSMCs). A, Cell growth curve of *circ_Lrp6*-silenced VSMCs transfected with a miR-145 inhibitor (i145; n=5). **B**, Migration evaluated by scratch assay of *circ_Lrp6*-silenced (shC5) VSMCs transfected with the miR-145 inhibitor (i145; n=8). Scale bar: 250 μm. **C**, Expression of actin (*Acta2*) and transgelin (*Sm22*) in *circ_Lrp6*-silenced VSMCs (shC5) transfected with i145, measured by reverse transcription quantitative polymerase chain reaction (RT-qPCR). **D**, Expression analysis of miR-145 targets regulated at the RNA level in *circ_Lrp6*-silenced VSMCs transfected with i145, measured by RT-qPCR. **E**, Expression of miR-145 targets in VSMCs overexpressing *circ_Lrp6*, measured by RT-qPCR. **F**, Growth curve of VSMCs overexpressing *circ_Lrp6*. **H**, Migration evaluated by scratch assay of *circ_Lrp6*-overexpressing VSMCs (n=5). Where not stated, data are the average of at least 3 independent experiments and error bars represent SD. For **A**, **B**, and **H**, data normality was calculated with Kolmogorov-Smirnov (K-S) test. To compare means, 1-way ANOVA was used in A–C, and 2-tailed Student *t* test was used in **D** and **E**; #*P*<0.05.

Lox (lysyl oxidase),[32,33] and *Yes1* (YES proto-oncogene 1)[34,35] (Figure 6D). By contrast, overexpression of *circ_Lrp6* increased the expression of the miR-145-regulated targets *fascin*, *Lox*, and *Yes1* (Figure 6E); coherently with the down-regulation of miR-145,[9] proliferative and migratory capacities of VSMCs were positively modulated (Figure 6F and 6H).

To determine whether levels of *circ_Lrp6* and miR-145 are inversely correlated, we assessed their expression in VSMCs stimulated for growth and differentiation. Specific treatments of VSCMs with cytokines revealed that PDGF (platelet-derived growth factor)-BB and TGF (transforming growth factor) β—2 key cytokines affecting VSMC differentiation[36] (Online Figure XIIA and XIIB)—downregulated *circ_Lrp6* after 24 hours. However, in PDGF-BB stimulated cells, *circ_Lrp6* expression followed that of miR-145 (Figure 7A; Online Figure XIIC), whereas in TGF-β-treated cells, there was an inverse correlation between *circ_Lrp6* and miR-145 expression (Figure 7B; Online XIID). *Lpr6*, the host gene, was regulated similarly to *circ_Lrp6* in both conditions (Online Figure XIIE and XIIF).

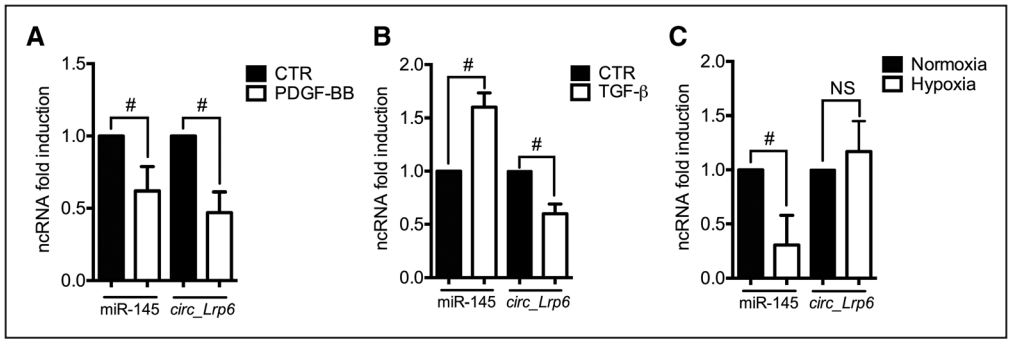

Figure 7. Biological regulation of circ_Lrp6 and miR-145 in vascular smooth muscle cells (VSMCs). **A** and **B**, *circ_Lrp6* and miR-145 expression in, respectively, PDGF (platelet-derived growth factor)-BB- and TGF (transforming growth factor)-β-treated VSMCs 24 h post-treatment, measured by reverse transcription quantitative polymerase chain reaction (RT-qPCR; n=5). **C**, Analysis of *circ_Lrp6* and miR-145 levels in VSMCs grown under hypoxic conditions (1% O_2) for 24 h and measured by RT-qPCR (n=5). Where not stated, data are the average of independent experiments and error bars represent SD. Data normality was calculated with Kolmogorov-Smirnov (K-S) test. To compare means, 2-tailed Student *t* test was used; #P<0.05. NS indicates not statistically significant.

We then wondered if *circ_Lrp6* and miR-145 expressions were altered with pathology. Among the conditions known to modulate VSMC biology, hypoxia contributes to the pathogenesis of vascular diseases, such as atherosclerosis and aortic aneurysms, among others.[37,38] Thus, we evaluated whether a reduced O_2 level differentially modulated the 2 ncRNAs. We found that hypoxia was associated with strongly downregulated miR-145, but that *circ_Lrp6* expression did not change (Figure 7C).

These findings suggest that interaction between circ_Lrp6 and miR-145 modulates the activity of the miRNA according to its level of expression.

Circ_Lrp6 in Vascular Diseases

To evaluate whether *circ_Lrp6* and miR-145 are differently regulated in vascular pathologies, we measured their levels in different pathological conditions: aortic samples derived from apolipoprotein E (ApoE) knockout mice following either a normal chow diet or a hypercholesterolemic Western diet, the latter a model of atherosclerosis[39]; aortic arches from transaortic constricted mice, a model of pressure overload heart failure[40]; and abdominal aortas of mice subjected to 2-kidney, 1-clip surgery, which develop systemic hypertension in a time-dependent manner.[41]

In atherosclerotic vessels, miR-145 expression was reduced (Figure 8A), as previously reported[4]; however, although expression of the host gene *Lrp6* was reduced (Online Figure XIIIA), the level of *circ_Lrp6* was not significantly modulated (Figure 8B). This finding indicated that in complex pathologies such as atherosclerosis, in which PDGF-BB- and hypoxia-induced pathways are largely involved,[42,43] the 2 ncRNAs are dissociated in terms of gene expression.

Similarly, while miR-145 was strongly downregulated in aorta from transaortic constricted mice (Figure 8C), *circ_Lrp6* (Figure 8D) as well as *Lrp6* (Online Figure XIIIB) were not. By contrast, in the aortas of hypertensive mice (Online Figure XIVA), miR-145 was upregulated, already at 2 weeks postsurgery (Figure 8E), while *circ_Lrp6* and *Lrp6* were not modulated (Figure 8F; Online Figure XIVB). Because the TGF-β pathway is involved in the development of hypertension,[44] the expression of miR-145 in hypertensive aortas was indeed in line with what we observed in vitro (Figure 7B). However, also these findings indicate that *circ_Lrp6* expression is less affected in the more complex in vivo condition as compared with the in vitro setting.

The importance of these findings was assessed for humans, measuring the expression of *circ_LRP6* in aneuryzed vessels. A small cohort of 7 patients presenting with an aneurysm at the level of the popliteal artery was studied. In all pathological vessels, we observed a significant reduction of miR-145 expression (Figure 8G), while *circ_LRP6* remained stable (Figure 8H).

Finally, based on these observations, we aimed to assess whether *circ_Lrp6* modulation might impact the pathological response in a murine model of vascular injury. To test this hypothesis, we examined the antiproliferative effect of specifically knocking down *circ_Lrp6* in a model of stenosis induced by perivascular carotid collar placement in $ApoE^{-/-}$ mice.[9] We performed systemic delivery of scrambled shRNA (shSCR) or circ_Lrp6-shRNA (shC5) viruses (Online Figure XVA), and determined the effects on the vessels 4 weeks after collar placement. Stented carotids treated with a control virus showed strong intimal hyperplasia, whereas delivery of the circ_Lrp6-shRNA virus markedly decreased the neointimal area (Figure 8I; Online Figure XVB through XVD).

Altogether, these findings indicate that the 2 ncRNAs are differently modulated in vascular pathologies in murine and human disease conditions and that the modulation of *circ_Lrp6* might impact the development of vascular diseases.

Discussion

Progresses in high-throughput sequencing and bioinformatics over the last decade have dramatically improved our knowledge on ncRNAs: circRNAs, once considered rare or an artifact of transcription,[45] are now classified as a category of ncRNAs.[46,47] CircRNAs may have higher sequence conservation in mammalian orthologues compared with other types of long ncRNAs, the fraction of mouse circRNAs having human orthologues ranging widely from 5% to 30%.[48,49]

Several circRNAs have already been identified as important for vascular biology.[50] Two, in particular, were found in VSMCs: circ_ANRIL (circular antisense noncoding RNA in the INK4 locus)[51] and circ_ACTA2 (Nrg-1-ICD induced

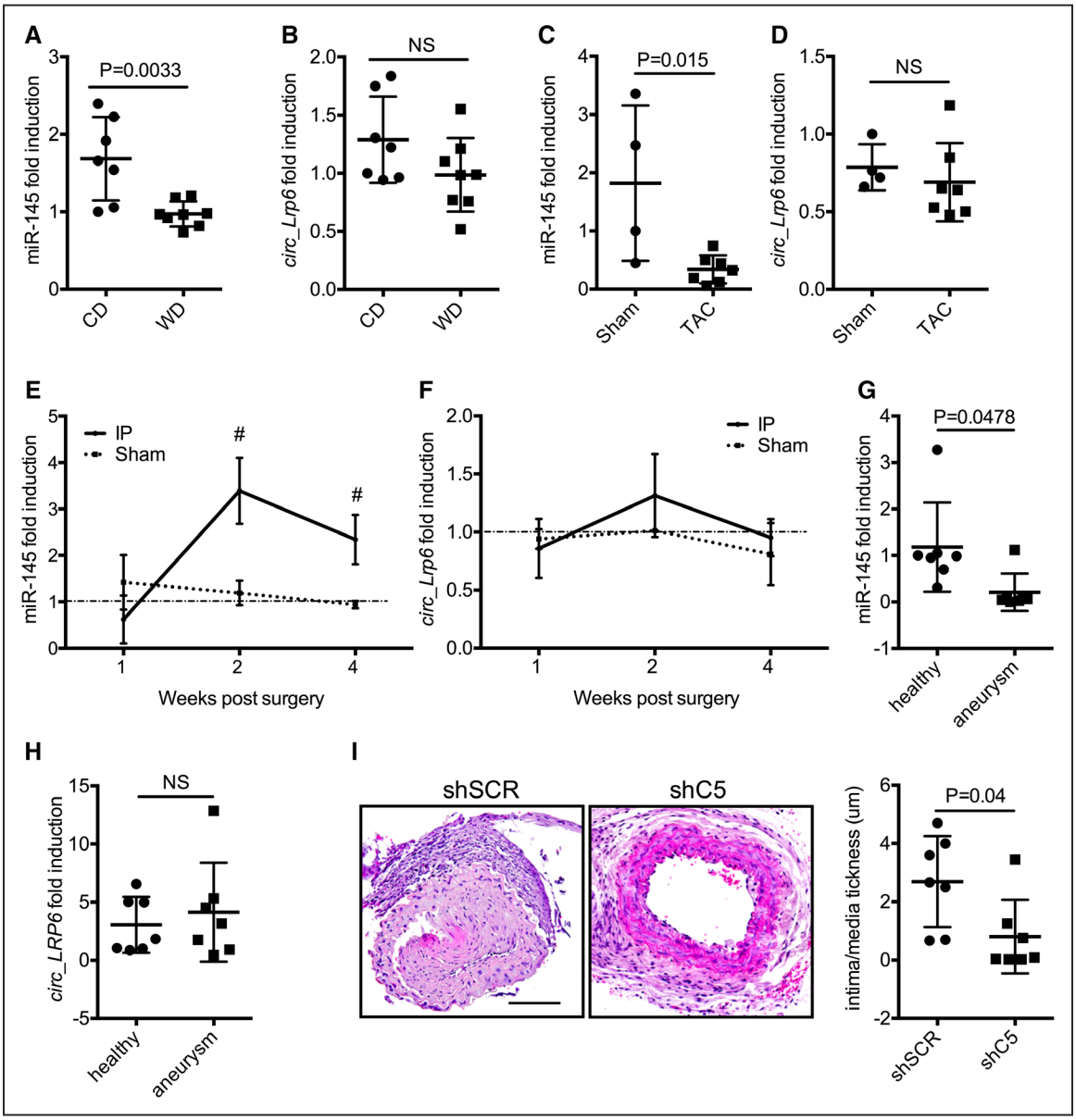

Figure 8. Circ_Lrp6 expression and modulation in diseased tissues. A and **B**, miR-145 and *circ_Lrp6* expression in aortas derived from ApoE$^{-/-}$ mice fed a normal chow diet (CD) or a hypercholesterolemic Western diet (WD) for 8 wk. Error bars represent SD (CD: n=7; for WD n=8). **C** and **D**, miR-145 and *circ_Lrp6* expression in aortic arch of mice with transaortic constriction (TAC) or subjected to a sham procedure. Error bars represent SD (sham: n=4; TAC: n=7). **E** and **F**), miR-145 and *circ_Lrp6* expression in aortas derived from hypertensive and sham-operated mice. Error bars represent SD (n=5). **G** and **H**, miR-145 and *circ_LRP6* expression in aneurytic human popliteal arteries and relative controls. Error bars represent SD (healthy: n=7; aneurysm: n=7). **I**, Representative hematoxylin/eosin staining of carotid sections of ApoE$^{-/-}$ mice infused with shSCR or shC5 viruses undergoing collar placement, and quantification, error bars represent SD (shSCR: n=7; shC5: n=7). Scale bar: 100 μm. Data normality was calculated with Kolmogorov-Smirnov (K-S) test. To compare means, an unpaired 2-tailed Student *t* test was used in **A**–**D**, and I, 1-way ANOVA in **E** and **F**, Mann-Whitney *U* test in **G**, and Wilcoxon test in **H**; #P<0.05, NS indicates not statistically significant.

circular ACTA2).[52] The former, originating from a gene localized at 9p21, has a variant associated with increased risk of coronary artery disease.[53] The latter binds to miR-548f-5p, modulating its activity by acting as a sponge; however, miR-548f-5p belongs to a poorly conserved primate-specific miRNA family that is not specific to VSMCs[54] and is involved in the regulation of migration and proliferation of cancer cells.[55]

To date, a comprehensive description of circRNAs expressed in VSMC is not available. Here, we list a large number of novel circRNAs expressed in VSMCs, demonstrating the function of one of them, circ_Lrp6, which interacts and modulates the activity of miRNA-145, a miRNA enriched in smooth muscle cells. Our findings indicate that miR-145 binds to and is modulated by circ_Lrp6. Of note, the level of this circRNA was stable in the disease conditions assessed by us. The only setting in which we found *circ_Lrp6* to be downmodulated was in vitro exposure to PDGF-BB, a stimulus that concomitantly lowered the intracellular level of miR-145. We found miR-145 was downregulated also in all the in vivo pathological conditions tested. It is, therefore, possible that circ_Lrp6 buffers miR-145 activity when this miRNA is above a certain level of expression. Our results led us to calculate that

≈25% of miR-145 might be bound to circ_Lrp6 under physiological conditions. Thus, it seems that circ_Lrp6 fine-tunes the activity of miR-145 by sequestering a significant amount of it. However, the effect of circ_Lrp6 in buffering miR-145 is probably aided by colocalization in specific subcellular compartments.[56,57] Indeed, our findings indicate that the 2 ncRNAs are positioned prevalently in P-bodies, cytoplasmic loci in which miRNAs exert their inhibitory activity on gene targets.[30] What function of miR-145 is affected—whether translation inhibition of target mRNAs or mRNA degradation—is a matter of speculation at this point.

It is of interest that this miR-145-binding circRNA is an alternatively spliced variant of the mRNA of a gene specifying for an LDL receptor, the role of which is well known in atherosclerosis.[58,59] Results of gain- and loss-of-function experiments clearly demonstrate the role of circ_Lrp6 in regulating the phenotype of VSMCs through miR-145 binding: in fact, in *circ_Lrp6*-silenced cells the concomitant inhibition of miR-145 reverted the effects of *circ_Lrp6* reduction, pointing toward a critical role of the miR-145 sponge activity of circ_Lrp6.

Nonetheless, other possible mechanisms of action cannot be excluded. CircRNAs have been shown to modulate gene expression by regulating transcription through interaction with polymerase II.[18] More recently, circRNAs were shown to possess open reading frames at the head-to-tail junction, leading to translation and protein generation.[60,61] Bioinformatics analysis of circ_Lrp6 identified a putative open reading frame deriving from the tail-to-head alternative splicing (data not shown). Thus, we cannot exclude that, similarly to the linear transcript myoregulin in skeletal muscle,[62] also circ_Lrp6 generates a protein affecting VSMC activity.

Finally, a search for single nucleotide polymorphisms on LRP6 led to the identification of 4 in the human gene. It is possible that a specific haplotype reflects in a differential expression of *circ_LRP6* and, thus, of differential miR-145-sponge activity. Further studies are needed to verify this possibility. The sequence homology between human and mouse circ_Lrp6, as well as its conservation throughout species, is nonetheless suggestive of a role of this ncRNA in human biology and disease.

The above findings add another layer of complexity to the mechanism through which miRNAs are regulated in VSMCs. Further studies are needed to define the different roles played by circRNAs in vascular diseases.

Acknowledgments

We thank Christina Pagiatakis for technical support with Northern blot experiments, and Alessandro Tarditi and Karolina Malik for human sample collection.

Sources of Funding

This work was supported by the following grants: European Research Council Advanced Grant (CardioEpigen, number 294609), Italian Ministry of Health (PE-2013-02356818), the CARIPLO Foundation (2015-0573), the Italian Ministry of Education, University and Research (2015583WMX), Progetto d'Interesse Invecchiamento (CNR-MIUR), and the EXPERT project of the ERANET-CVD research programme (Italian Ministry of Health) to G. Condorelli; Italian Ministry of Health (GR-2013-02355011) and Fondazione Veronesi to L. Elia.

Disclosures

None.

References

1. Thum T, Condorelli G. Long noncoding RNAs and microRNAs in cardiovascular pathophysiology. *Circ Res*. 2015;116:751–762. doi: 10.1161/CIRCRESAHA.116.303549
2. Elia L, Condorelli G. RNA (Epi)genetics in cardiovascular diseases. *J Mol Cell Cardiol*. 2015;89:11–16. doi: 10.1016/j.yjmcc.2015.07.012
3. Condorelli G, Latronico MV, Cavarretta E. microRNAs in cardiovascular diseases: current knowledge and the road ahead. *J Am Coll Cardiol*. 2014;63:2177–2187. doi: 10.1016/j.jacc.2014.01.050
4. Elia L, Quintavalle M, Zhang J, Contu R, Cossu L, Latronico MV, Peterson KL, Indolfi C, Catalucci D, Chen J, Courtneidge SA, Condorelli G. The knockout of miR-143 and -145 alters smooth muscle cell maintenance and vascular homeostasis in mice: correlates with human disease. *Cell Death Differ*. 2009;16:1590–1598. doi: 10.1038/cdd.2009.153
5. Xin M, Small EM, Sutherland LB, Qi X, McAnally J, Plato CF, Richardson JA, Bassel-Duby R, Olson EN. MicroRNAs miR-143 and miR-145 modulate cytoskeletal dynamics and responsiveness of smooth muscle cells to injury. *Genes Dev*. 2009;23:2166–2178. doi: 10.1101/gad.1842409
6. Boettger T, Beetz N, Kostin S, Schneider J, Krüger M, Hein L, Braun T. Acquisition of the contractile phenotype by murine arterial smooth muscle cells depends on the Mir143/145 gene cluster. *J Clin Invest*. 2009;119:2634–2647. doi: 10.1172/JCI38864
7. Cordes KR, Sheehy NT, White MP, Berry EC, Morton SU, Muth AN, Lee TH, Miano JM, Ivey KN, Srivastava D. miR-145 and miR-143 regulate smooth muscle cell fate and plasticity. *Nature*. 2009;460:705–710. doi: 10.1038/nature08195
8. Quintavalle M, Elia L, Condorelli G, Courtneidge SA. MicroRNA control of podosome formation in vascular smooth muscle cells in vivo and in vitro. *J Cell Biol*. 2010;189:13–22. doi: 10.1083/jcb.200912096
9. Elia L, Kunderfranco P, Carullo P, Vacchiano M, Farina FM, Hall IF, Mantero S, Panico C, Papait R, Condorelli G, Quintavalle M. UHRF1 epigenetically orchestrates smooth muscle cell plasticity in arterial disease. *J Clin Invest*. 2018;128:2473–2486. doi: 10.1172/JCI96121
10. Hergenreider E, Heydt S, Tréguer K, Boettger T, Horrevoets AJ, Zeiher AM, Scheffer MP, Frangakis AS, Yin X, Mayr M, Braun T, Urbich C, Boon RA, Dimmeler S. Atheroprotective communication between endothelial cells and smooth muscle cells through miRNAs. *Nat Cell Biol*. 2012;14:249–256. doi: 10.1038/ncb2441
11. Climent M, Quintavalle M, Miragoli M, Chen J, Condorelli G, Elia L. TGFβ triggers miR-143/145 transfer from smooth muscle cells to endothelial cells, thereby modulating vessel stabilization. *Circ Res*. 2015;116:1753–1764. doi: 10.1161/CIRCRESAHA.116.305178
12. Elia L, Quintavalle M. Epigenetics and vascular diseases: influence of non-coding RNAs and their clinical implications. *Front Cardiovasc Med*. 2017;4:26. doi: 10.3389/fcvm.2017.00026
13. Vicens Q, Westhof E. Biogenesis of circular RNAs. *Cell*. 2014;159:13–14. doi: 10.1016/j.cell.2014.09.005
14. Memczak S, Jens M, Elefsinioti A, et al. Circular RNAs are a large class of animal RNAs with regulatory potency. *Nature*. 2013;495:333–338. doi: 10.1038/nature11928
15. Zhang XO, Wang HB, Zhang Y, Lu X, Chen LL, Yang L. Complementary sequence-mediated exon circularization. *Cell*. 2014;159:134–147. doi: 10.1016/j.cell.2014.09.001
16. Jeck WR, Sorrentino JA, Wang K, Slevin MK, Burd CE, Liu J, Marzluff WF, Sharpless NE. Circular RNAs are abundant, conserved, and associated with ALU repeats. *RNA*. 2013;19:141–157. doi: 10.1261/rna.035667.112
17. Zhang Y, Zhang XO, Chen T, Xiang JF, Yin QF, Xing YH, Zhu S, Yang L, Chen LL. Circular intronic long noncoding RNAs. *Mol Cell*. 2013;51:792–806. doi: 10.1016/j.molcel.2013.08.017
18. Li Z, Huang C, Bao C, et al. Exon-intron circular RNAs regulate transcription in the nucleus. *Nat Struct Mol Biol*. 2015;22:256–264. doi: 10.1038/nsmb.2959
19. Ivanov A, Memczak S, Wyler E, Torti F, Porath HT, Orejuela MR, Piechotta M, Levanon EY, Landthaler M, Dieterich C, Rajewsky N. Analysis of intron sequences reveals hallmarks of circular RNA biogenesis in animals. *Cell Rep*. 2015;10:170–177. doi: 10.1016/j.celrep.2014.12.019
20. Hansen TB, Jensen TI, Clausen BH, Bramsen JB, Finsen B, Damgaard CK, Kjems J. Natural RNA circles function as efficient microRNA sponges. *Nature*. 2013;495:384–388. doi: 10.1038/nature11993
21. Li Y, Zheng Q, Bao C, Li S, Guo W, Zhao J, Chen D, Gu J, He X, Huang S. Circular RNA is enriched and stable in exosomes: a

promising biomarker for cancer diagnosis. *Cell Res*. 2015;25:981–984. doi: 10.1038/cr.2015.82
22. Cheng J, Metge F, Dieterich C. Specific identification and quantification of circular RNAs from sequencing data. *Bioinformatics*. 2016;32:1094–1096. doi: 10.1093/bioinformatics/btv656
23. Farina FM, Inguscio A, Kunderfranco P, Cortesi A, Elia L, Quintavalle M. MicroRNA-26a/cyclin-dependent kinase 5 axis controls proliferation, apoptosis and in vivo tumor growth of diffuse large B-cell lymphoma cell lines. *Cell Death Dis*. 2017;8:e2890. doi: 10.1038/cddis.2017.291
24. Ballantyne MD, Pinel K, Dakin R, et al. Smooth muscle enriched long noncoding RNA (SMILR) regulates cell proliferation. *Circulation*. 2016;133:2050–2065. doi: 10.1161/CIRCULATIONAHA.115.021019
25. Dobin A, Davis CA, Schlesinger F, Drenkow J, Zaleski C, Jha S, Batut P, Chaisson M, Gingeras TR. STAR: ultrafast universal RNA-seq aligner. *Bioinformatics*. 2013;29:15–21. doi: 10.1093/bioinformatics/bts635
26. Schmied C, Steinbach P, Pietzsch T, Preibisch S, Tomancak P. An automated workflow for parallel processing of large multiview SPIM recordings. *Bioinformatics*. 2016;32:1112–1114. doi: 10.1093/bioinformatics/btv706
27. Pruitt KD, Tatusova T, Brown GR, Maglott DR. NCBI Reference Sequences (RefSeq): current status, new features and genome annotation policy. *Nucleic Acids Res*. 2012;40:D130–D135. doi: 10.1093/nar/gkr1079
28. Quintavalle M, Condorelli G, Elia L. Arterial remodeling and atherosclerosis: miRNAs involvement. *Vascul Pharmacol*. 2011;55:106–110. doi: 10.1016/j.vph.2011.08.216
29. Suzuki H, Zuo Y, Wang J, Zhang MQ, Malhotra A, Mayeda A. Characterization of RNase R-digested cellular RNA source that consists of lariat and circular RNAs from pre-mRNA splicing. *Nucleic Acids Res*. 2006;34:e63. doi: 10.1093/nar/gkl151
30. Liu J, Valencia-Sanchez MA, Hannon GJ, Parker R. MicroRNA-dependent localization of targeted mRNAs to mammalian P-bodies. *Nat Cell Biol*. 2005;7:719–723. doi: 10.1038/ncb1274
31. Owens GK. Regulation of differentiation of vascular smooth muscle cells. *Physiol Rev*. 1995;75:487–517. doi: 10.1152/physrev.1995.75.3.487
32. Liep J, Kilic E, Meyer HA, Busch J, Jung K, Rabien A. Cooperative effect of miR-141-3p and miR-145-5p in the regulation of targets in clear cell renal cell Carcinoma. *PLoS One*. 2016;11:e0157801. doi: 10.1371/journal.pone.0157801
33. Kothapalli D, Liu SL, Bae YH, Monslow J, Xu T, Hawthorne EA, Byfield FJ, Castagnino P, Rao S, Rader DJ, Puré E, Phillips MC, Lund-Katz S, Janmey PA, Assoian RK. Cardiovascular protection by ApoE and ApoE-HDL linked to suppression of ECM gene expression and arterial stiffening. *Cell Rep*. 2012;2:1259–1271. doi: 10.1016/j.celrep.2012.09.018
34. Gregersen LH, Jacobsen AB, Frankel LB, Wen J, Krogh A, Lund AH. MicroRNA-145 targets YES and STAT1 in colon cancer cells. *PLoS One*. 2010;5:e8836. doi: 10.1371/journal.pone.0008836
35. Huang TC, Renuse S, Pinto S, Kumar P, Yang Y, Chaerkady R, Godsey B, Mendell JT, Halushka MK, Civin CI, Marchionni L, Pandey A. Identification of miR-145 targets through an integrated omics analysis. *Mol Biosyst*. 2015;11:197–207. doi: 10.1039/c4mb00585f
36. Owens GK, Kumar MS, Wamhoff BR. Molecular regulation of vascular smooth muscle cell differentiation in development and disease. *Physiol Rev*. 2004;84:767–801. doi: 10.1152/physrev.00041.2003
37. Kasivisvanathan V, Shalhoub J, Lim CS, Shepherd AC, Thapar A, Davies AH. Hypoxia-inducible factor-1 in arterial disease: a putative therapeutic target. *Curr Vasc Pharmacol*. 2011;9:333–349.
38. Sluimer JC, Daemen MJ. Novel concepts in atherogenesis: angiogenesis and hypoxia in atherosclerosis. *J Pathol*. 2009;218:7–29. doi: 10.1002/path.2518
39. Sala F, Aranda JF, Rotllan N, Ramírez CM, Aryal B, Elia L, Condorelli G, Catapano AL, Fernández-Hernando C, Norata GD. MiR-143/145 deficiency attenuates the progression of atherosclerosis in Ldlr-/-mice. *Thromb Haemost*. 2014;112:796–802. doi: 10.1160/TH13-11-0905
40. Elia L, Contu R, Quintavalle M, Varrone F, Chimenti C, Russo MA, Cimino V, De Marinis L, Frustaci A, Catalucci D, Condorelli G. Reciprocal regulation of microRNA-1 and insulin-like growth factor-1 signal transduction cascade in cardiac and skeletal muscle in physiological and pathological conditions. *Circulation*. 2009;120:2377–2385. doi: 10.1161/CIRCULATIONAHA.109.879429
41. Lorenz JN, Lasko VM, Nieman ML, Damhoff T, Prasad V, Beierwaltes WH, Lingrel JB. Renovascular hypertension using a modified two-kidney, one-clip approach in mice is not dependent on the α1 or α2 Na-K-ATPase ouabain-binding site. *Am J Physiol Renal Physiol*. 2011;301:F615–F621. doi: 10.1152/ajprenal.00158.2011
42. Heldin CH, Westermark B. Mechanism of action and in vivo role of platelet-derived growth factor. *Physiol Rev*. 1999;79:1283–1316. doi: 10.1152/physrev.1999.79.4.1283
43. Sano H, Sudo T, Yokode M, Murayama T, Kataoka H, Takakura N, Nishikawa S, Nishikawa SI, Kita T. Functional blockade of platelet-derived growth factor receptor-beta but not of receptor-alpha prevents vascular smooth muscle cell accumulation in fibrous cap lesions in apolipoprotein E-deficient mice. *Circulation*. 2001;103:2955–2960.
44. Goumans MJ, Liu Z, ten Dijke P. TGF-beta signaling in vascular biology and dysfunction. *Cell Res*. 2009;19:116–127. doi: 10.1038/cr.2008.326
45. Hsu MT, Coca-Prados M. Electron microscopic evidence for the circular form of RNA in the cytoplasm of eukaryotic cells. *Nature*. 1979;280:339–340.
46. Dixon RJ, Eperon IC, Hall L, Samani NJ. A genome-wide survey demonstrates widespread non-linear mRNA in expressed sequences from multiple species. *Nucleic Acids Res*. 2005;33:5904–5913. doi: 10.1093/nar/gki893
47. Tan WL, Lim BT, Anene-Nzelu CG, Ackers-Johnson M, Dashi A, See K, Tiang Z, Lee DP, Chua WW, Luu TD, Li PY, Richards AM, Foo RS. A landscape of circular RNA expression in the human heart. *Cardiovasc Res*. 2017;113:298–309. doi: 10.1093/cvr/cvw250
48. Guo JU, Agarwal V, Guo H, Bartel DP. Expanded identification and characterization of mammalian circular RNAs. *Genome Biol*. 2014;15:409. doi: 10.1186/s13059-014-0409-z
49. Rybak-Wolf A, Stottmeister C, Glažar P, et al. Circular RNAs in the mammalian brain are highly abundant, conserved, and dynamically expressed. *Mol Cell*. 2015;58:870–885. doi: 10.1016/j.molcel.2015.03.027
50. Boeckel JN, Jaé N, Heumüller AW, Chen W, Boon RA, Stellos K, Zeiher AM, John D, Uchida S, Dimmeler S. Identification and characterization of hypoxia-regulated endothelial circular RNA. *Circ Res*. 2015;117:884–890. doi: 10.1161/CIRCRESAHA.115.306319
51. Holdt LM, Stahringer A, Sass K, et al. Circular non-coding RNA ANRIL modulates ribosomal RNA maturation and atherosclerosis in humans. *Nat Commun*. 2016;7:12429. doi: 10.1038/ncomms12429
52. Sun Y, Yang Z, Zheng B, Zhang XH, Zhang ML, Zhao XS, Zhao HY, Suzuki T, Wen JK. A novel regulatory mechanism of smooth muscle α-Actin expression by NRG-1/circACTA2/miR-548f-5p axis. *Circ Res*. 2017;121:628–635. doi: 10.1161/CIRCRESAHA.117.311441
53. Schunkert H, König IR, Kathiresan S, et al; Cardiogenics; CARDIoGRAM Consortium. Large-scale association analysis identifies 13 new susceptibility loci for coronary artery disease. *Nat Genet*. 2011;43:333–338. doi: 10.1038/ng.784
54. Liang T, Guo L, Liu C. Genome-wide analysis of mir-548 gene family reveals evolutionary and functional implications. *J Biomed Biotechnol*. 2012;2012:679563. doi: 10.1155/2012/679563
55. Fang L, Zhang HB, Li H, Fu Y, Yang GS. miR-548c-5p inhibits proliferation and migration and promotes apoptosis in CD90(+) HepG2 cells. *Radiol Oncol*. 2012;46:233–241. doi: 10.2478/v10019-012-0025-z
56. Han D, Li J, Wang H, Su X, Hou J, Gu Y, Qian C, Lin Y, Liu X, Huang M, Li N, Zhou W, Yu Y, Cao X. Circular RNA circMTO1 acts as the sponge of microRNA-9 to suppress hepatocellular carcinoma progression. *Hepatology*. 2017;66:1151–1164. doi: 10.1002/hep.29270
57. Zheng Q, Bao C, Guo W, Li S, Chen J, Chen B, Luo Y, Lyu D, Li Y, Shi G, Liang L, Gu J, He X, Huang S. Circular RNA profiling reveals an abundant circHIPK3 that regulates cell growth by sponging multiple miRNAs. *Nat Commun*. 2016;7:11215. doi: 10.1038/ncomms11215
58. Mani A, Radhakrishnan J, Wang H, Mani A, Mani MA, Nelson-Williams C, Carew KS, Mane S, Najmabadi H, Wu D, Lifton RP. LRP6 mutation in a family with early coronary disease and metabolic risk factors. *Science*. 2007;315:1278–1282. doi: 10.1126/science.1136370
59. Keramati AR, Singh R, Lin A, Faramarzi S, Ye ZJ, Mane S, Tellides G, Lifton RP, Mani A. Wild-type LRP6 inhibits, whereas atherosclerosis-linked LRP6R611C increases PDGF-dependent vascular smooth muscle cell proliferation. *Proc Natl Acad Sci USA*. 2011;108:1914–1918. doi: 10.1073/pnas.1019443108
60. Legnini I, Di Timoteo G, Rossi F, Morlando M, Briganti F, Sthandier O, Fatica A, Santini T, Andronache A, Wade M, Laneve P, Rajewsky N, Bozzoni I. Circ-ZNF609 is a circular RNA that can be translated and functions in myogenesis. *Mol Cell*. 2017;66:22.e9–37.e9. doi: 10.1016/j.molcel.2017.02.017
61. Pamudurti NR, Bartok O, Jens M, et al. Translation of CircRNAs. *Mol Cell*. 2017;66:9.e7–21.e7. doi: 10.1016/j.molcel.2017.02.021
62. Anderson DM, Anderson KM, Chang CL, Makarewich CA, Nelson BR, McAnally JR, Kasaragod P, Shelton JM, Liou J, Bassel-Duby R, Olson EN. A micropeptide encoded by a putative long noncoding RNA regulates muscle performance. *Cell*. 2015;160:595–606. doi: 10.1016/j.cell.2015.01.009